Angular dependent interatomic potential for Ti-V system for molecular dynamics simulations

Angular dependent interatomic potential for Ti-V system for molecular dynamics simulations

Andrey I. Kartamyshev[1,2] ‡, Alexey G. Lipnitskii[3], Anton O. Boev[3], Ivan V. Nelasov[3,4], Vyacheslav N. Maksimenko[3], Dmitriy A. Aksyonov[5], Truong Khang Nguyen [1,2]

[1]Division of Computational Physics, Institute for Computational Science, Ton Duc Thang University, Ho Chi Minh City, Vietnam
[2]Faculty of Electrical & Electronics Engineering, Ton Duc Thang University, Ho Chi Minh City, Vietnam
[3]The Center of Nanostructured Materials and Nanotechnologies, Belgorod State University, Belgorod, Russian Federation
[4]Institute of Problems of Chemical Physics, Russian Academy of Sciences, Chernogolovka, Moscow oblast, 142432 Russia
[5]Skolkovo Institute of Science and Technology, 121205 Moscow, Russian Federation

E-mail: kartamyshevandrey@tdtu.edu.vn (Andrey I. Kartamyshev)

E-mail: lipnitskii@bsu.edu.ru (Alexey G. Lipnitskii)

E-mail: nelasow@bsu.edu.ru (Ivan V. Nelasov)

E-mail: nguyentruongkhang@tdtu.edu.vn (Truong Khang Nguyen)

Abstract. An interatomic potential for the Ti-V binary alloy focusing on the evolution of defects, including ones arising as a result of the irradiation process, was constructed within the Lipnitskii-Saveliev approach, which accurately takes into account three-particle interactions and the sum of all multi-particle interactions of a higher order in the framework of the centrally symmetric approximation. In the new potential, Ti-V interactions were fitted to the DFT data on a set of model structures with different coordination numbers, including ones with vacancies. The properties used for fitting are accurately reproduced by the present potentials for both pure elements and alloy systems. The potential was tested on the binding energies between Ti atoms and self-point defects in bcc V, elastic moduli, thermal expansion and melting point of some alloys, and diffusion. We obtained qualitative agreement for these properties with available theoretical and experimental data. Finally, we investigated the evolution of excess vacancies in the V-4 at. % Ti alloy at 700 K, which are typical conditions of vanadium-based alloys for fusion applications. We found that no vacancy loop is formed in the alloy in contrast to the pure V, which agrees with the experimental observations. The potential is expected to be especially suitable for irradiation simulations of vanadium-based V-Ti alloys.

Keywords: Ti-V, interatomic potentials, molecular dynamics, point defects, binding energy, diffusion.

Submitted to: *Modelling Simulation Mater. Sci. Eng.*

‡ Corresponding author at: Ton Duc Thang University, Ho Chi Minh City, Vietnam (Andrey I. Kartamyshev)

1. Introduction

Vanadium-titanium based alloys are considered as a candidate material for the first wall of fusion reactors because of the improved combination of chemical and mechanical properties in comparison with steels or composites based on silicon [1, 2, 3, 4]. It is experimentally established, that Ti addition in the concentration 4-5% is needed to improve a radiation-resistant property of pure vanadium through reducing the void swelling [5]. Experimental studying of the atomic processes is very complicated and can provide only a limited amount of data, which is why computer modeling methods are widely used by researchers in the world.

There are two commonly used approaches for modeling on the atomic-scale level. Firstly, the density functional theory (DFT) methods are employed to investigate the properties of the atomic systems by taking into account the electronic structure. They were used to research the possible ways of Ti influence on point defects in the bcc lattice of vanadium. Boev et al. [6] studied the interaction of Ti atoms with vacancies and self-interstitial atoms, while authors of [7] conducted research of their interaction with H and He in bcc V matrix. However, DFT methods have several limitations. Namely, they allow to conduct simulations of relatively small samples ($\sim$ 1000 atoms), and calculations of the time evolution for larger cells will require significant computational time. In turn, molecular dynamics (MD) is one of the most promising tools for studying the alloying effect on the properties at relevant temperatures for larger atomic systems. MD allows to simulate dynamic processes such as a primary radiation cascade or an evolution of excess vacancy structure to understand the causes of the effect of an alloying element on radiation resistance of a material. The reliability of the MD simulations depends completely on the employed interatomic potentials.

There are several potentials for the Ti-V system, which are the embedded atom method (EAM) potential [8], two modified MEAM potentials [9, 10], improved Finnis-Sinclair potential [11] and our previous one [12] developed within the Lipnitskii-Saveliev (LS) approach [13]. Feng et al. developed the interatomic potential [9], which correctly reproduces structural and energetic properties of ZnS- and NaCl-type structures (TiV) as well as D03-type (Ti_3V and TiV_3). However, its fitting database does not contain bcc solid solution structures, as well as information about the quality of the description of point defects and their complexes in the Ti-V alloys. The potential of Yang et al. [10] was constructed as part of the higher-order potential to study the behavior of atoms of light elements (H, He, C, and O) in alloys of the Ti-V system and does not contain information about the interaction of Ti atoms with point defects in bcc lattice of V. In addition, the potentials for pure Ti [14] and V [15], employed for the construction of the binary one, underestimate the melting point for both elements. In turn, the improved Finnis-Sinclair (IFS) Ti-V potential developed by Fu et al. [11] as part of V-Ti-Cr system accurately predicts structural and elastic properties of Ti solid solution in bcc lattice of V; however, detailed characterization of interactions between alloying elements and self-point defects (both vacancies and self-interstitial atoms) was not presented.

Our previously developed interatomic potential for the Ti-V system (will be denoted as POT_TiV_old) was tested in the previous works [16, 12, 17, 18]. POT_TiV_old showed a good qualitative description of properties at the relevant temperatures and the cascade conditions. However, recently we constructed a new potential for pure Ti [19], which demonstrates the improved description of phonon, elastic, defect and thermal properties in comparison with the previous one [12].

In the present work, the interatomic potential for Ti-V binary system based on potentials for pure Ti and V was constructed within the LS approach [13]. The potentials for V-V and Ti-Ti interactions are presented in detail in our previous works [13], which was also included in the POT_TiV_old potential, and [19], respectively. Both potentials are able to correctly reproduce properties of the ideal lattices, point defects, as well as thermal ones, especially thermal expansion and melting, which are very important for the description of diffusion properties and, as consequence, the evolution of defects in these materials. In the present paper, all MD simulations were performed utilizing our developed software package, which was successfully applied in our previous works, including ones devoted to the development of the interatomic potentials for pure Ti [19] and V [13], the binary Ti-V [12] and V-W [20] systems, investigation of the diffusion in tungsten [21], and simulation of the cascades of atomic displacements in the V-Ti alloys [18]. Generalization of the LS approach to the case of multi-component systems is defined in Section 2. Section 3 describes the fitting database and optimization procedure, the optimized Ti-V potentials' functions, as well as the fitting accuracy. In Section 4, tests of the constructed Ti-V potential including energetic characteristics of point defect complexes, melting and diffusion properties, which were not included in the fitting procedure, will be presented. Our results and discussion on possible applications of the potentials are summarized in Section 5.

2. Methods

2.1. LS potential model

The LS method [13, 19], used in this work, represents the effective potential energy E_{pot}, defined as the series of n-body interactions, by the sum of three terms:

$$E_{pot} = \sum_{i<j}^{N} \Phi_{ji}(R_{ji}) + \sum_{i}^{N} \sum_{k<j\neq i}^{N} \sum_{p,q}^{n_3} g_i^{pq}(cos(\theta_{jik}))\times \\ \times f_{ji}^{p}(R_{ji}) f_{ki}^{q}(R_{ki}) + \sum_{i}^{N} F_i(\bar{\rho}_i), \quad (1)$$

where

$$\bar{\rho}_i = \sum_{j\neq i} \rho_{ji}(R_{ji}). \quad (2)$$

In Eq.(1) the first term describes the pair interactions $\Phi_{ji}(R_{ji})$ between atoms j and i separated by a distance R_{ji} and depends on their sorts. The second term describes the 3-body interactions, where $f_{ji}^{p}(R_{ji})$ are the basis functions depending on the interatomic distances, and n_3 is the number of these functions; they depend on sorts of atoms j and i with the condition $f_{ji}^{p}(R_{ji}) \neq f_{ij}^{p}(R_{ij})$. The functions $g_i^{pq}(cos(\theta_{jik}))$ depend on the angles θ_{jik} between the bonds ji and ki around the i atom and its sort. The third term in Eq.(1) is the effective representation of the sum of n-body interactions ($n > 3$), defined by function $F_i(\bar{\rho}_i)$ within the centrally symmetric approximation (CSA), and depends on sort of atom i. Finally, $\rho_{ji}(R_{ji})$ in Eq. (2) are the basis functions for description of all n-body interactions with $n > 3$; they depend on sorts of atoms j and i with the condition $\rho_{ji}(R_{ji}) \neq \rho_{ij}(R_{ij})$.

We will denote functions $\Phi_{ji}(R_{ji})$, $\rho_{ji}(R_{ji})$, $F_i(\bar{\rho}_i)$, $f_{ji}^{p}(R_{ji})$, and $g_i^{pq}(x)$ as the potential functions. As follows from the Eq.(1), to describe interatomic interactions in the binary system Ti-V, it is necessary to have the potential functions of Ti-Ti and V-V interactions, as well as ones for Ti-V interactions.

2.2. DFT calculations

For our calculations we used density functional theory (DFT) [22, 23] method within projected augmented wave (PAW) formalism [24] and supercell approach using ABINIT package [25] to calculate target values for the fitting database and the Vienna ab initio simulation package (VASP) [26] through management package SIMAN [27] to calculate values for testing the interatomic potential. In the PAW-potentials for titanium and vanadium, $3s$, $3p$, $4s$ and $3d$ electrons are considered as valence in both used packages. All chosen potentials were constructed within the generalized gradient approximation (GGA) of Perdew-Burke-Ernzerhof (PBE) functional [28].

ABINIT parameters. The kinetic energy cutoff of the plane wave basis set of 860 eV was chosen. Smoothing the Fermi level was carried out by the method of Methfessel-Paxton[29] with a smearing width of 0.136 eV. Mesh of k-points, constructed using the Monkhorst-Pack method [30], with size of $14 \times 14 \times 14$ was chosen for the bcc structure of vanadium. The corresponding density of k-points was used for all other structures. DFT calculations were carried out to achieve the convergence criterion of energy 10^{-6} eV and maximum forces less than 10 meV/Å.

VASP parameters. The cutoff energy of the plane-wave basis set was chosen as 350 eV. Smoothing the Fermi level was carried out by the method of Methfessel-Paxton[29] with a smearing width of 0.2 eV. Mesh of k-points, constructed using the Monkhorst-Pack method [30], with size of $11 \times 11 \times 11$ was chosen for the bcc structure of vanadium. The corresponding density of k-points was used for all other structures. Equilibrium self-point defect (SPD) configurations and their complexes with Ti atoms in bcc V were determined using the full relaxation method until the maximum forces acting on atoms in a simulation cell become less than 25 meV/Å.

To confirm the validity of the chosen parameters we performed calculations of convergence of formation enthalpy and maximum force acting on atoms for TiV compound with the B_2 structure with respect to the cutoff energy and size of the k-points grid. We used a 2-atom unit cell with ideal positions of atoms for the formation enthalpy and with vanadium atom displaced along the [100] direction by ~ 0.015 Å. Results of calculations are presented on figure 1. It demonstrates that at chosen parameters' sets the convergence is reached in all cases; in ABINIT and VASP, the formation enthalpies (forces acting on atoms) are calculated with an accuracy of ~ 2 meV/atom and ~ 10 meV/atom (~ 5 meV/Å and ~ 30 meV/Å), respectively.

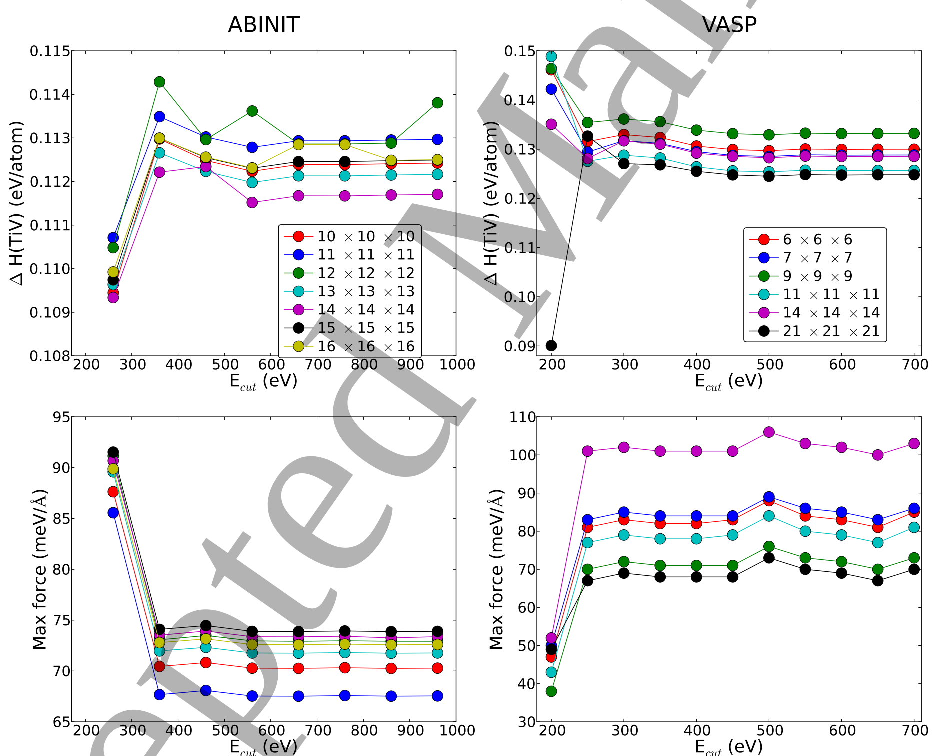

Figure 1. Results of DFT convergence calculations of formation enthalpy and maximum force acting on atoms in the TiV compound with the B_2 structure in dependence on cutoff energy and size of k-points grid performed employing ABINIT (**a** and **c**) and VASP (**b** and **d**) packages. For calculations of the forces, vanadium atom was displaced along the [100] direction by ~ 0.015 Å.

2.3. Ti-SPD binding energy

The defect formation energies and binding energies of the Ti-SPD complexes are calculated using the following equations [6]:

$$E_f^{Vac} = E^{Vac}(V_{N-1}) - [(N-1)/N]E(V_N), \tag{3}$$

$$E_f^{SIA} = E^{SIA}(V_{N+1}) - [(N+1)/N]E(V_N), \tag{4}$$

and

$$E_b^{(A,B)} = E^A(\mathrm{V}_{N-1} + A) + E^B(\mathrm{V}_{N-1} + B) - E^{A+B}(\mathrm{V}_{N-2} + A + B) - E(\mathrm{V}_N), \tag{5}$$

where E_f^{Vac} and E_f^{SIA} are the formation energies of vacancy and self-interstitial atom (SIA), respectively; $E(V_N)$ is the energy of the ideal bcc supercell with N vanadium atoms, $E^{Vac}(V_{N-1})$ is one of the supercell with vacancy, and $E^{SIA}(V_{N+1})$ is one of the supercell with SIA; $E_b^{(A,B)}$ is the binding energy between two defects ($A, B =$ Ti atom, SIA or vacancy), $E^A(V_{N-1} + A)$ and $E^B(V_{N-1} + B)$ are the energies of the supercells with corresponding types of point defects, and lastly $E^{A+B}(V_{N-2} + A + B)$ is the energy of supercell, containing both point defects.

Calculations of these energies were performed for 250-site (5×5×5 two-atom bcc unit cells) and 2000-site (10×10×10 two-atom bcc unit cells) supercells using molecular static method until forces acting on atoms are less than 0.001 meV/Å.

2.4. Melting point

We performed calculations of the melting point for series of alloys, for which temperatures of liquidus and solidus almost coincide (60-80 at. % Ti) according to the thermodynamic assessment of the Ti-V phase diagram [31]. This allowed us to employ the approximation of the composition equality of liquid and solid phases. For each concentration, three initial samples with a different random distribution of Ti atoms were used. The melting temperature was calculated using an NPH ensemble (at a constant number of atoms, pressure, and enthalpy of a system) [32] for a 19652-atom simulation supercell (17×17×34 two-atom bcc unit cells) consisting of solid bcc and liquid phases in contact with each other (the co-existence method). Simulations were performed for 450 ps with a time step of 3 fs. For each concentration, three samples with a random distribution of Ti atoms in a sample were constructed; for each sample, sixteen supercells with different starting temperatures were employed.

2.5. Diffusion

Vacancy diffusion in bcc V-4Ti lattice was simulated by molecular dynamics method using an NPT ensemble (at a constant number of particles, pressure, and temperature), in which pressure and temperature were kept employing Berendsen barostat [33] and Nose-Hoover thermostat [34] respectively, at a series of temperatures between 600 and 1900 K with a step of 100 K. The simulation time equals 8 ns with a time step of 2 fs. Each modeled sample is a 2000-site bcc supercell with 50 randomly distributed atoms and 1 vacancy. Diffusion coefficient D was calculated as a function of the temperature for a fixed concentration of vacancies, according to the expression:

$$D = (1/6N)(dZ/dt), \tag{6}$$

where Z is the sum of the squares of atomic displacements of N atoms at time t. dZ/dt is calculated as the slope of linear approximation of the $Z(t)$ dependence. The diffusion activation energy for a fixed vacancy concentration is equal to the effective vacancy migration energy by the vacancy diffusion mechanism.

The activation energy of vacancy migration E_v^m was obtained by:

$$D(T) = D_0 exp\left(\frac{-E_v^m}{kT}\right). \tag{7}$$

where the symbols k and T are the Boltzmann constant and the absolute temperature, respectively.

3. Ti-V potential construction

Phase diagram of the Ti-V system demonstrates that there are solid solution phases only [31] above temperature of 473 K in all concentration range. Titanium and vanadium form a complete series of solid solutions with bcc lattice at elevated temperatures above ≈ 1150 K. Below this temperature, vanadium is slightly soluble in hexagonal close-packed (hcp) Ti (about 3.1 at. % V at ~ 790 K). The solubility of titanium in bcc vanadium gradually decreases to about 9.8 at. % Ti as temperature reduces from 1150 K to 473 K.

3.1. Fitting database

Potential parameters were optimized to describe the fitting database of DFT data. The optimization procedure was presented in detail in [13].

DFT database consists of formation enthalpies and atomic volumes for seventeen model solid solutions with the bcc structure, as well as compounds TiV, compounds TiV_3 and Ti_3V, and compounds TiV_2 and Ti_2V with structures, B_2, $L1_2$, and C_{32}, respectively. Marked twenty-two model structures are sampled atomic configurations with titanium concentrations from 6.25 at.% to 93.75 at.%. In addition, two samples of solid solutions of V in hcp and C_{32} Ti (corresponding to the V concentration ~ 0.03 %) were included in the fitting database. To improve the description of point defect complexes in bcc V, six samples with Ti-vacancy complexes were also employed in the fitting procedure; this group of samples consists of five Ti-monovacancy complexes and one Ti-divacancy complex. The equilibrium lattice parameters were determined by fitting the dependence of atomic energy on volume $E(V)$ to the equation of state of the form[35] for the bcc, B_2 and $L1_2$ structures. For the bcc structure, the volume relaxation was also employed. For the C_{32} structure, we calculated the dependency of atomic energy on the lattice parameters $E(a, c)$ for a grid of points, followed by finding its minimum. For the bcc structure (ideal and with Ti-vacancy complexes) 16-site supercell ($2 \times 2 \times 2$ elementary cubic 2-atom cells) was used. Structures C_{32}, $L1_2$ and B_2 were sampled employing 3-atom, 4-atom and 2-atom cells, respectively.

The formation enthalpy of the compounds in the Ti-V system ($\Delta H(Ti_mV_n)$) is calculated using the following formula:

$$\Delta H(Ti_mV_n) = \frac{H(Ti_mV_n) - (mH_{hcp}^{Ti} + nH_{bcc}^{V})}{m+n}, \tag{8}$$

where $H(Ti_mV_n)$ is the enthalpy of a Ti_mV_n compound with $n+m$ atoms, mH_{hcp}^{Ti} is the one of m titanium atoms in equilibrium hcp structure, and nH_{bcc}^{V} is the one of n vanadium atoms in equilibrium bcc structure.

3.2. Potential functions

For a complete description of the interatomic interactions in the Ti-V system, it is necessary to describe the interactions of Ti-Ti, V-V, and Ti-V. The first one is described by the potential functions for titanium, published in our recent paper [19]. V-V interactions are described by potential functions for vanadium, published by Lipnitskii and Saveliev [13].

To complete the interatomic potential, it is necessary to describe the cross-Ti-V interactions by construction of the following potential functions: $\Phi_{12}(r)$, two functions

$\rho_{ji}(r)$ ($\rho_{12}(r)$ and $\rho_{21}(r)$), and four functions $f^p_{ji}(r)$ ($f^1_{12}(r)$, $f^2_{12}(r)$, $f^1_{21}(r)$ and $f^2_{21}(r)$). The results of the optimization of the potential parameters for Ti-V system are presented in the figure 2 in graphical form. The potential functions are presented in the form of cubic splines, knots of which are the potential parameters.

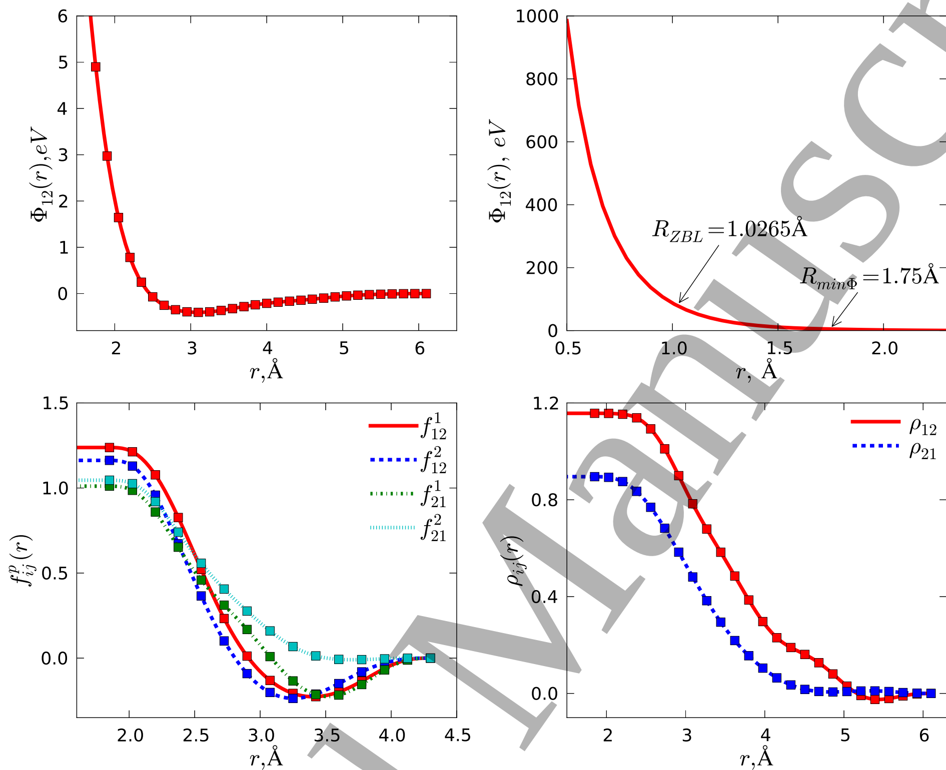

Figure 2. Potential functions $\Phi_{12}(r)$ (in eV), $\rho_{ji}(r)$ (dimensionless), $f^p_{ji}(r)$ (dimensionless) of the Ti-V interactions in form of cubic splines. The values of the functions at the nodes splines (the potential parameters) are denoted by squares. The functions $f^p_{ji}(r)$ and $\rho_{ji}(r)$ are constant at $r < R_{min}$. The pair potential $\Phi_{12}(r)$ at $r < R_{ZBL}$ has the form of the universal ZBL screening function [36] and is a continuous function along with its first and second derivatives in the interval $[R_{ZBL}, R_{min\Phi}]$. Ti-Ti and V-V potential functions are presented in [19] and [13], respectively.

Thirty spline knots were used for the function Φ_{12} on the interval $[R_{min\Phi}, R_\Phi]$, twenty-five spline knots for the function ρ_{12} and ρ_{21} on the interval $[R_{min}, R_\Phi]$ and fifteen spline knots for the function f^1_{12}, f^2_{12}, f^1_{21} and f^2_{21} on the interval $[R_{min}, R_f]$. The inner cutoff radius for the function Φ_{12} equals to $R_{min\Phi} = 1.75$ Å. It was selected as the average value $R_{min\Phi}$ of the potential for pure titanium ($R_{min\Phi} = 1.7$ Å[19]) and vanadium ($R_{min\Phi} = 1.8$ Å[13]). The inner cutoff radius for the functions ρ_{12}, ρ_{12}, f^1_{12}, f^2_{12}, f^1_{21} and f^2_{21} equals to $R_{min} = 1.85$ Å. It was selected as the average value R_{min} of the potential for pure titanium ($R_{min} = 1.9$ Å[19]) and vanadium ($R_{min} = 1.8$ Å[13]). The outer cutoff radius for the pair potential Φ_{12} and functions ρ_{12} and ρ_{21} is $R_\Phi = 6.1$ Å, which is equal to the average value of the values R_Φ of the potentials for pure titanium ($R_\Phi = 6.4$ Å[19]) and vanadium ($R_\Phi = 5.8$ Å[13]). The outer cutoff radius $R_f = 4.3$ Å for the functions f^1_{12}, f^2_{12}, f^1_{21} and f^2_{21}, which is the average value of values R_f of the potentials for pure titanium ($R_f = 4.5$ Å[19]) and vanadium ($R_f = 4.1$ Å[13]). According to our works [13, 19], the potential functions f^p_{ji} and ρ_{ji} are constant below R_{min}, and the function Φ_{12} is a Coulomb screened pair potential in Ziegler-Biersack-Littmark (ZBL) form [36] below R_{ZBL} with parameters E_{ZBL} and R_{ZBL} equal to -9.36 eV and 1.0265 Å, respectively. Between R_{ZBL} and $R_{min\Phi}$, the potential function Φ_{12} is described as a fifth-degree polynomial function; the chosen parameters of the ZBL model ensure continuity of Φ_{12} and its two derivatives. The values of the potential functions of Ti-V in the spline knots, which are optimized parameters of the potential, are presented in table 1. Parameters η_e and η_r, used to solve the problem of incompatibility between the DFT and experimental quantities for the POT_TiV potential, were determined by linear interpolation from the quantities for pure titanium (1.000 and 1.006, respectively[19]) and vanadium (0.90 and 1.005, respectively [13]) (for more details, see Section 3.1 in [13]).

Table 1. Parameters specifying the seven cubic splines that comprise the Ti-V interaction part of the Ti-V potential. The first part of the table lists the number of knots N for each spline, and the range of the spline variables at t_{min} as well as t_{max}. The middle part of the table gives the values at equally spaced spline knots defined by $t_i = t_{min} + (i-1) \cdot (t_{max} - t_{min})/(N-1)$.

i	t	t_{min}	t_{max}	N			
Φ_{12}	r(Å)	1.75	6,1	30			
ρ_{12}	r(Å)	1.85	6.1	25			
ρ_{21}	r(Å)	1.85	6.1	25			
f^1_{12}	r(Å)	1.85	4.3	15			
f^2_{12}	r(Å)	1.85	4.3	15			
f^1_{21}	r(Å)	1.85	4.3	15			
f^2_{21}	r(Å)	1.85	4.3	15			
i	$\Phi_{12}(r_i)$ (eV)	$\rho_{12}(r_i)$	$\rho_{21}(r_i)$	$f^1_{12}(r_i)$	$f^2_{12}(r_i)$	$f^1_{21}(r_i)$	$f^2_{21}(r_i)$
1	4.89945371	1.15727550	0.89547741	1.23817649	1.16240748	1.01104165	1.04601059
2	2.97086133	1.15678163	0.89265451	1.21300317	1.12909915	0.98629375	1.02561916
3	1.64218155	1.15340328	0.87529033	1.07720594	0.95792630	0.85919545	0.91970995
4	0.78075229	1.13852285	0.83467496	0.82658142	0.67194501	0.65202973	0.74052292
5	0.24578894	1.09264990	0.76892782	0.52149296	0.36569442	0.45882181	0.55753271
6	-0.07090975	1.01022495	0.68241501	0.23266844	0.10120502	0.31120726	0.40604952
7	-0.25281977	0.89968787	0.58356610	0.01178745	-0.09117544	0.16836590	0.27669028
8	-0.34887621	0.78339676	0.48126686	-0.13114419	-0.20197707	0.00880167	0.16007433
9	-0.39429245	0.67932427	0.38302573	-0.20733785	-0.23682937	-0.13393998	0.06780002
10	-0.40609335	0.58327646	0.29446415	-0.22676897	-0.21147647	-0.21482858	0.01329956
11	-0.39477190	0.48499264	0.21846331	-0.19884246	-0.14970208	-0.21731132	-0.00728426
12	-0.36526470	0.38615452	0.15551805	-0.13580146	-0.08077147	-0.15541781	-0.00887193
13	-0.32382406	0.29682139	0.10458563	-0.06045289	-0.02913491	-0.06898338	-0.00421306
14	-0.28075093	0.22995443	0.06451076	-0.01021073	-0.00429175	-0.01156653	-0.00071398
15	-0.24241705	0.18966671	0.03521402	0.00000000	0.00000000	0.00000000	0.00000000
16	-0.21098407	0.16121086	0.01686151				
17	-0.18573892	0.12658391	0.00802275				
18	-0.16430292	0.08061355	0.00604600				
19	-0.14371412	0.03018740	0.00781041				
20	-0.12129113	-0.00867228	0.01012119				
21	-0.09691881	-0.02441100	0.01049508				
22	-0.07270405	-0.02106434	0.00792247				
23	-0.05123809	-0.01019344	0.00360146				
24	-0.03445487	-0.00180793	0.00060675				
25	-0.02244834	0.00000000	0.00000000				
26	-0.01407830						
27	-0.00794093						
28	-0.00321001						
29	-0.00050075						
30	0.00000000						

3.3. Fitting accuracy

The fitting results of formation enthalpies (calculated using Eq. (8)) and equilibrium volumes for the series of Ti-V structures, which include model bcc and hcp solid solutions, stoichiometric compounds with C_{32}, $L1_2$, B_2 structures as well as configurations with Ti-vacancy complexes (see details in Section 3.1 Fitting procedure), are presented in figure 3. They demonstrate that the atomic volumes are reproduced closer to the DFT target values than the formation enthalpies; their average deviations are equal to 1.9 % (maximum value of 10.7 %) and 6.7 % (maximum value of 14.7 %), respectively. It should be noted that the average deviations for structures with defects do not exceed corresponding values for the full fitting database (0.3 % and 5.7 % for the atomic volumes and formation enthalpies, respectively). Therefore, we can expect the correct reproduction of the interaction between titanium atoms and vacancies in the bcc lattice of vanadium.

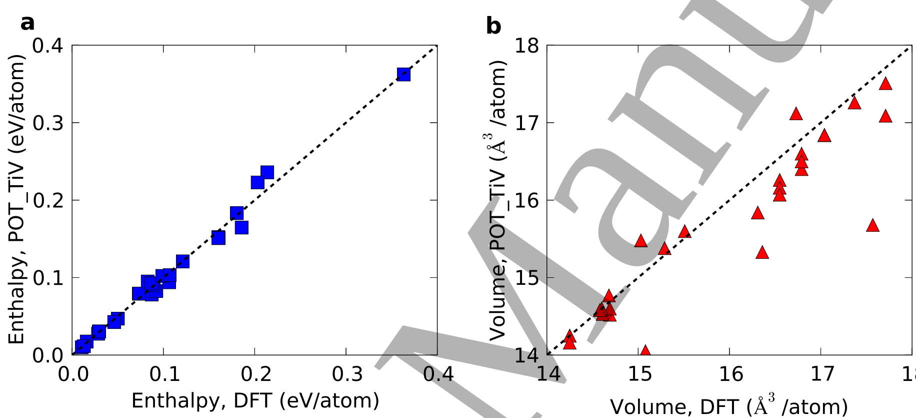

Figure 3. Scatter plots for (a) enthalpies of mixing and (b) atomic volumes for the series of Ti-V model structures with respect to the DFT database.

4. Tests of the binary potential

We assessed the performance of the POT_TiV potential by comparison of the calculated properties with known experimental and DFT data. These properties include lattice parameters, elastic moduli, complexes of point defects with Ti atoms, thermal expansion and melting points for the series of Ti-V alloys, and diffusion. Finally, the evolution of excess vacancies in the V-4Ti alloy in comparison with pure V was investigated and compared with the experimental observations. In this case, the initial vacancy concentration corresponds to one observed in defective regions, formed as a result of a cascade of atomic collisions caused by ion or neutron irradiation.

4.1. Lattice parameters and elastic moduli

Table 3. Lattice parameters of structures of the Ti-V system in comparison with our DFT results and known experimental data.

Parameter	POT_TiV	Exp.	DFT
	TiV (bcc)		
a, Å	3.147	3.150 [37], 3.136 [38]	3.124
	$Ti_2V(C_{32})$		
a, Å	4.508	4.562 [39]	4.532
c/a	0.593	0.608 [39]	0.593
	$TiV_2(C_{32})$		
a, Å	4.454	–	4.511
c/a	0.599	–	0.561

Table 3 shows lattice parameters of several Ti-V structures calculated with the POT_TiV potential and known experimental data. The results predicted by the POT_TiV potential deviate from the experimental data by less than 2.5%, which, along with good satisfactory agreement for values from fitting database, demonstrates its ability to reproduce structures with different coordination numbers and chemical composition.

Accurate description of the elastic constants allows to correctly reproduce the mechanical stability of a material, as well as strain fields around defects in it. Elastic moduli of the Ti-V structures compared to the DFT data are presented in table 4. For pure elements, satisfactory agreement between the POT_TiV potential and experiment (average deviations equal to $\sim$ 15.3 % and $\sim$ 0.9 % for Ti and V, respectively) is associated with their inclusion in the corresponding fitting databases [19, 13]. Elastic constants for model structures (TiV-B_2, Ti_2V-C_{32}, and TiV_2-C_{32}) demonstrate their mechanical stability, which is in qualitative agreement with the results of DFT calculations. It is important to determine the ability of the POT_TiV potential to reproduce elastic moduli for solid solution structures, which was done on the example of TiV_{15}-bcc (6.25 at. % Ti) alloy. We obtained an acceptable agreement with DFT and deduced experimental data [11] (12 % and 24 %, respectively), which ensures its mechanical stability. Better agreement for the IFS potential [11] can be attributed to the inclusion of these values into the optimization procedure.

Table 4. Elastic constants in units of GPa for pure Ti phases (hcp, bcc and C_{32}), pure V (bcc) and Ti-V phases (B_2, two $L1_2$ and two C_{32}) in comparison with the DFT fitting data and experiment.

	C_{11}	C_{12}	C_{44}	C_{33}	C_{13}
		Ti-hcp (hexagonal)			
POT_TiV	168	76	49	171	77
DFT [40]	176	84	45	191	75
Exp.(4 K) [41]	176	87	51	191	68
		Ti-bcc (cubic)			
POT_TiV	90	113	46	–	–
DFT [42]	87	116	41	–	–
Exp.(1293 K) [43]	134	110	36	–	–
		Ti-C_{32} (hexagonal)			
POT_TiV	219	87	66	254	84
DFT [42]	201	82	56	251	52
		V-bcc (cubic)			
POT_TiV	230	122	43	–	–
DFT [44]	258	142	20	–	–
Exp. [45]	230	120	43	–	–
		TiV-B_2 (cubic)			
POT_TiV	213	139	69	–	–
DFT	169	132	22	–	–
		Ti_2V-C_{32} (hexagonal)			
POT_TiV	315	173	53	390	139
DFT	162	126	22	190	101
		TiV_2-C_{32} (hexagonal)			
POT_TiV	221	172	18	187	105
DFT	215	129	56	106	99
		TiV_{15}-bcc (cubic)			
POT_TiV	213	139	69	–	–
DFT	255	148	79	–	–
IFS [11]	229	104	49	–	–
Exp. [11]	222	118	43	–	–

4.2. Ti-SPD binding energy

Table 5 shows the binding energies, E_b, between Ti atoms and self-point defects (SPD) (vacancy, divacancy and self-interstitial atom (SIA)) depending on the nearest neighbor(nn) position in bcc vanadium obtained using the POT_TiV and

POT_TiV_old potentials in comparison with the results of DFT calculated from Eq. 5 (see Section 2.3). Configurations of the Ti-SPD complexes are shown in figure 4.

Table 5. Binding energy E_b, eV between titanium atoms and self-point defect (Vacancy or SIA) depending on the nearest neighbor(nn) position in bcc vanadium. Data for POT_TiV_old (250/2000 atom cells), POT_TiV (250/2000 atom cells) and DFT (250 atom cell)

Defect	nn	POT_TiV_old	POT_TiV	DFT
Ti-Vacancy	1	0.64/–	0.51/0.50	0.37
	2	–0.03/–	-0.03/-0.03	–0.06
	3	–0.02/–	-0.02/-0.02	0.07
2Ti-Vacancy	1	*/*	0.41/0.41	*
	2	0.61/–	0.57/0.57	0.60
	3	1.34/–	0.90/0.91	0.75
	4	0.64/–	0.43/0.47	0.27
	5	1.45/–	1.00/0.99	0.80
Ti-Divacancy**	1	0.51/0.81	0.68/0.68	0.46
Ti - SIA$_{<111>}$	1	–/0.35	0.21/0.21	0.15
2Ti - SIA$_{<111>}$	1	–/0.69	–/0.32	0.29
	2	–/0.78	–/0.45	0.31
	3	–/0.62	–/0.46	0.35
3Ti - SIA$_{<111>}$	1	–/1.17	–/0.61	0.41
	2	–/1.13	–/1.00	0.46
	3	–/1.06	–/0.82	0.54

*-transformed into 2Ti-Vacancy(5)
**-binding energy between titanium atom and divacancy

As can be seen from table 5, the binding energy of complexes of point defects are in qualitative agreement with the results of DFT calculations. In particular, the POT_TiV potential correctly describes the binding between vacancy and Ti atom at the first nearest neighbor position, and the highest binding energy of the 2Ti-Vac (5) among 2Ti-Vac(i) (i=1-5) complexes. Moreover, we obtained good quantitative agreement for binding energy between the Ti atom and divacancy with a deviation of about 12 %. For complexes of Ti atoms with self-interstitials, the POT_TiV potential demonstrates satisfactory qualitative and even quantitative (in the case of Ti-SIA and

2Ti-SIA complexes, the average deviation of about 31 %) reproduction of binding energies with an average deviation of about 49%. It should be noted that the fitting database does not contain information about interactions between Ti atoms and self-interstitial atoms in bcc V.

The average deviation between POT_TiV and DFT results over all Ti-SPD complexes is about 49%. This difference can be associated with the fact that the fitting databases for the potentials of pure titanium [19] and vanadium [13] include experimental data, which show only qualitatively agreement with the DFT ones. For example, DFT value of 2.6 eV of the vacancy formation energy in vanadium [44] differs from the experimental one of 2.1 eV [46] by 0.5 eV. Therefore, this difference is also an estimate of DFT errors when calculating the binding energies of impurity atoms with a vacancy in bcc V.

Thus, the present POT_TiV potential is able to qualitatively describe interactions between Ti atoms and self-point defects in bcc V and shows improvement in reproduction of binding energies in comparison with the POT_TiV_old one.

4.3. Thermal expansion and melting point

The relative change of the lattice parameter of the V - 20 at. % Ti alloy (V-20Ti) on temperature was calculated using molecular dynamics simulations for an isobaric-isothermal ensemble (NPT) at zero pressure. In the NPT ensemble, the temperature was kept constant using Nose-Hoover thermostat [34] and pressure was kept constant using Berendsen barostat [33]. The calculations were performed using a 1024-atom bcc supercell with randomly distributed Ti atoms, which was gradually heated from 293 K to 1793 K with a temperature step of 15 K and annealing at each temperature during 100 ps. The MD calculated thermal expansion of the V-20Ti in comparison with experiment is shown in figure 5 and demonstrates almost perfect agreement with the experiment [47], especially for low temperatures, while for the elevated ones the POT_TiV underestimate this quantity.

The obtained melting temperatures are demonstrated in figure 6 in comparison with the corresponding part of the assessed phase diagram [31]. As we can see from this figure, the POT_TiV potential overestimates the melting temperature compared to the assessment by about 300 K, and the difference between the potential and assessment decreases as the concentration of Ti rises. The overestimation of the melting point may originate from the underestimation of the thermal expansion at high temperatures. Another possible cause of such difference can originate from the lack of electron effects. It was shown on the example of 3d transition metals that chemical bonding nature, in particular, bond overlap population, has a significant influence on melting points [48]. However, a detailed investigation of reasons underlying the calculated melting points overestimation is beyond the scope of this paper.

4.4. Diffusion

Diffusion coefficients in V and V-4Ti, calculated employing Eqs. (6) and (7) at fixed vacancy concentration as described in Section 2.5, are plotted in figure 7 as a function of inverse temperature. According to the figure, the activation energies for vacancy migration, determined by fitting to the Arrhenius equation in pure V and V-4Ti, are 0.52 ± 0.04 eV and 0.75 ± 0.03 eV, respectively. The value for pure V agrees with known experimental data (0.5-1.2 eV [49]) and with one obtained using drag method (0.49 eV

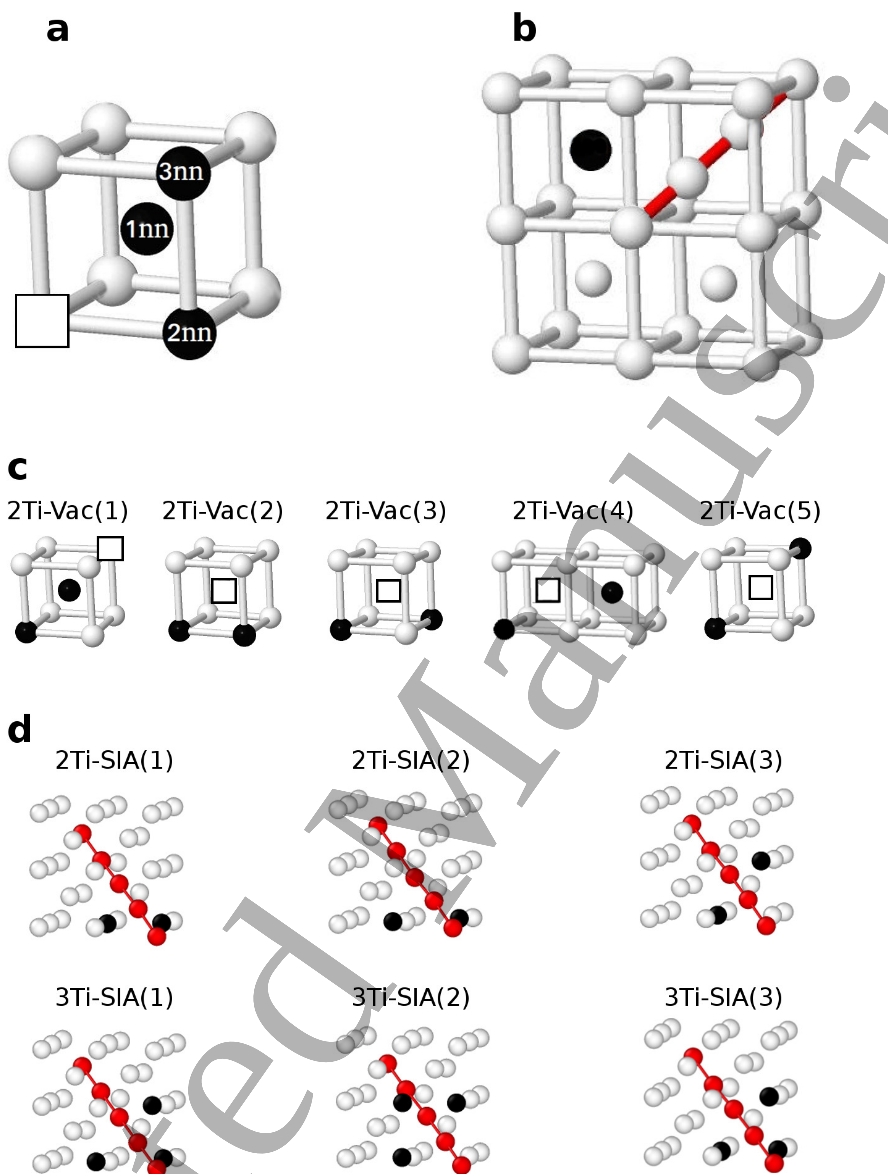

Figure 4. The considered nearest-neighboring (nn) atomic configurations: a) 1nn-3nn positions (black atoms) near the vacancy (white atom); b) Ti position near the ⟨111⟩ dumbbell highlighted with space diagonal; c) 2Ti-Vac(i) complexes, where i - nn Ti-Ti position; d) 2Ti-SIA and 3Ti-SIA complexes. Black - Ti, white - V, rectangle - vacancy, red - dumbbell ⟨111⟩.

[13]). In turn, for V-4Ti the POT_TiV potential shows higher vacancy diffusivity by 0.23 eV, which can be attributed to the attractive interaction between vacancies and Ti atoms. The obtained value is less than binding energy between Ti atom and vacancy

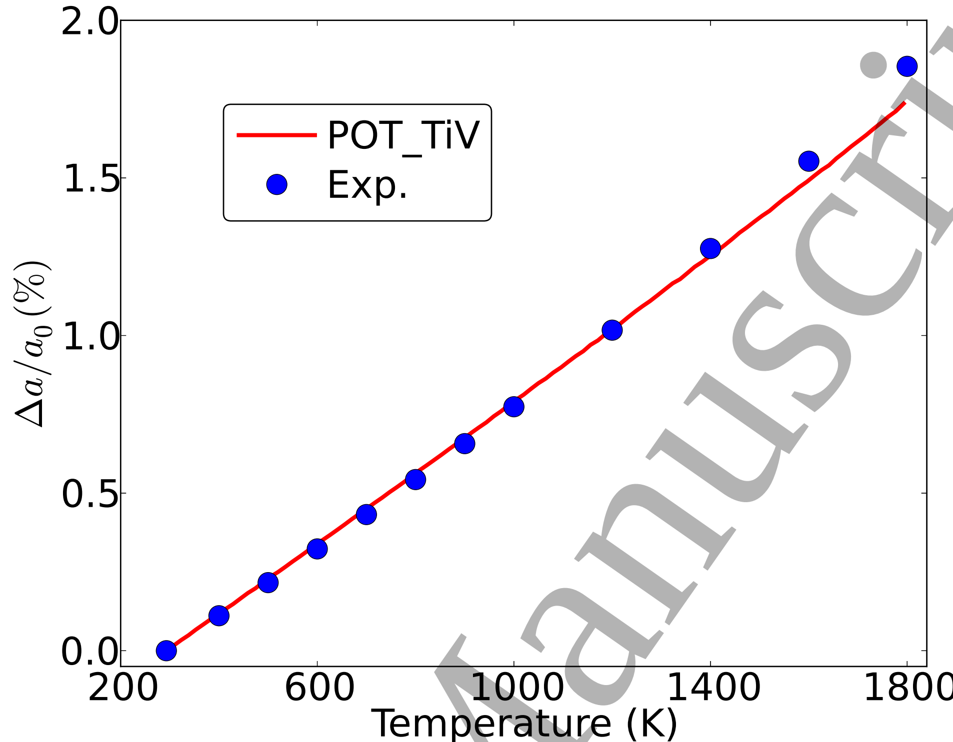

Figure 5. The relative change of the lattice parameter $\Delta a/a_0$ on temperature for the V-20 at. % Ti alloy with the bcc structure, calculated using the POT_TiV potential in comparison with the experimental measurements (Ref. [47]). a_0 is the lattice parameter at 293 K.

(0.5 eV, see table 5) probably due to the temperature effects. As we can see from figure 7, the difference in diffusivity between V and V-4Ti decreases as temperature rises, and two values almost coincide near the melting point of bcc V, meaning that binding between Ti atom and vacancy becomes weaker at high temperatures. However, a detailed investigation of the origins of this effect is beyond the scope of this paper.

4.5. Excess vacancies' evolution

It is known from experiments and MD simulations that highly mobile SIAs move to the periphery of the cascade region, while monovacancies (mostly) stay in the center of the defective region in the materials subjected to the ion or neutron irradiation [50, 17, 18]. Following Brommer et al. [51] and Fan et al. [52] we used 50 monovacancies per 2000-atom sample ($10\times10\times10$ two-atom bcc unit cells) as a starting configuration; this was shown to be a typical vacancy concentration caused by a cascade of atomic collisions. The evolution of the process was tracked using the dependencies of potential energy and volume of the sample on modeling time. The occurrence of the plateau in these dependencies indicates the finish of the process. MD simulations were performed at a temperature of 700 K for 16 ns. Visualization of the final structures was performed

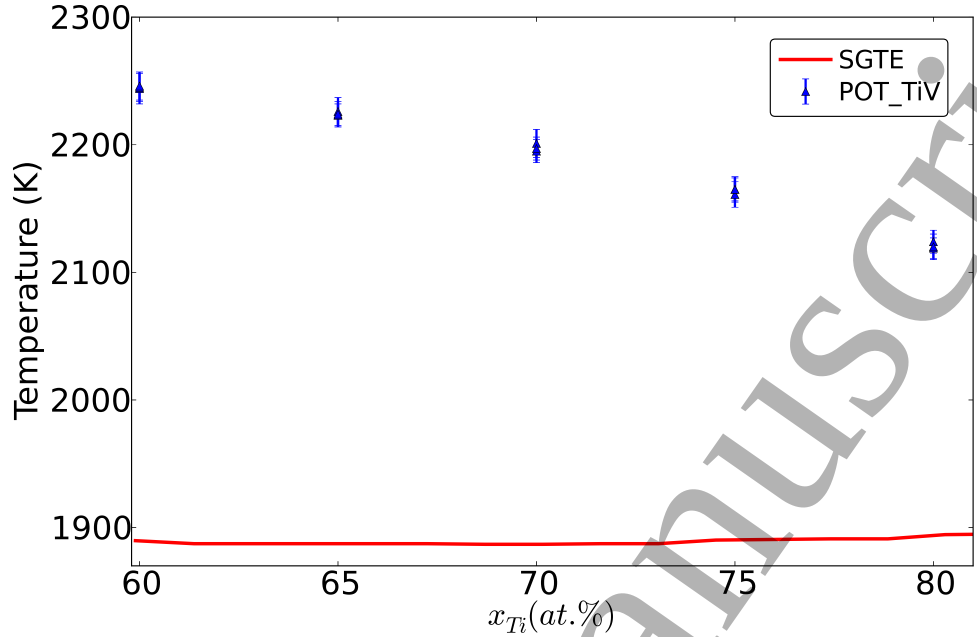

Figure 6. Melting temperatures of Ti-V alloys for the concentration range of 60-80 at. % Ti in comparison with a thermodynamic assessment of Ti-V phase diagram (SGTE) [31].

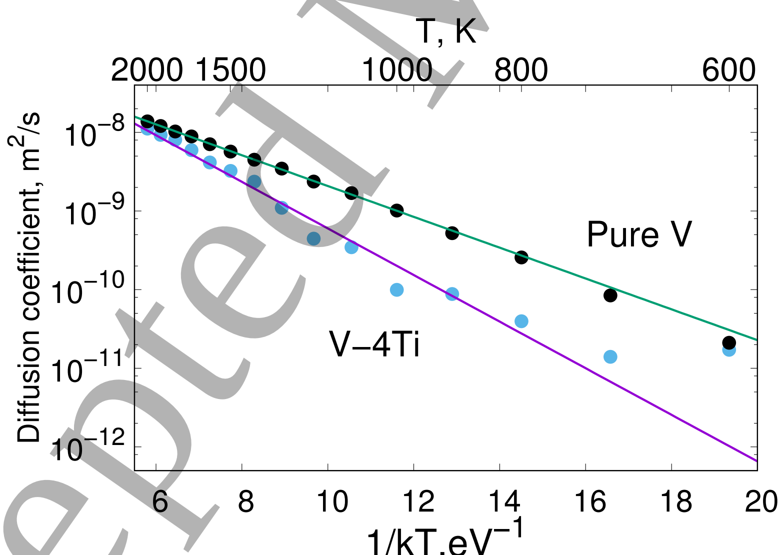

Figure 7. Temperature dependence of diffusion coefficients for pure V and the V-4Ti at fixed vacancy concentration calculated using MD simulations with the POT_TiV potential.

using the OVITO package [53].

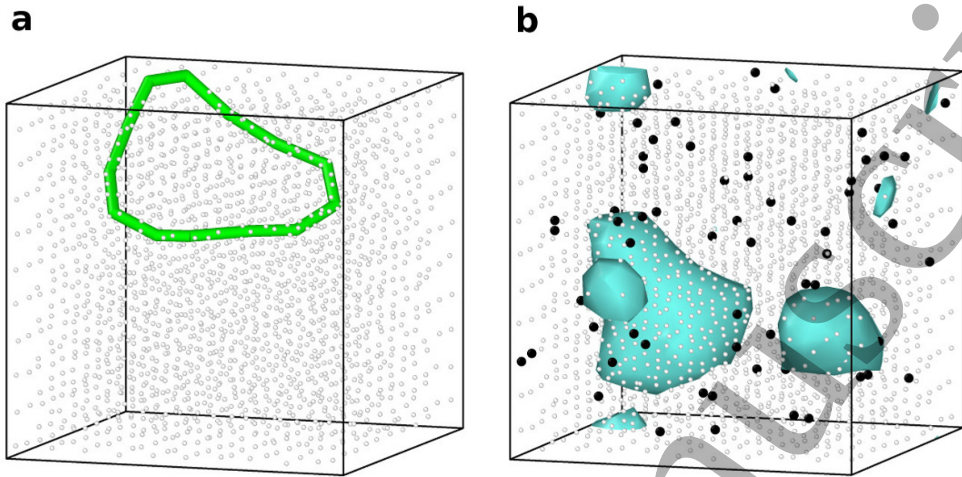

Figure 8. Structures of 50 excess vacancies modelled after 16 ns at 700 K using POT_TiV. a) pure V, b) V-4Ti. Here, grey spheres are vanadium atoms, black are the titanium ones, green line is the vacancy loop $1/2\langle 111\rangle$, and blue denote regions containing complexes of Ti atoms with vacancies.

Figure 8 shows that the vacancy loop is formed in pure vanadium during the simulation time. According to the dislocation analysis (DXA) implemented in OVITO package [54], it is the $1/2\ \langle 111\rangle$ vacancy loop, which is commonly found in the irradiated pure bcc vanadium [55, 56]. In turn, V-4Ti alloy does not contain any loops after the simulation, that agree with experimental results in V-5Ti alloy, in which only separate vacancies were observed [57].

5. Summary and conclusion

In the present paper, a new angular dependent interatomic potential for the binary Ti-V system was developed. It was constructed within the Lipnitskii-Saveliev (LS) approach, which allows to describe simultaneously structural, elastic, defect, thermal and phase transition properties in satisfactory agreement with known experimental and theoretical data. The present potential (POT_TiV) includes components for the Ti-Ti and V-V interactions, described in detail in our previous articles, as well as Ti-V ones developed within the current study. Fitting databases for the pure elements' potentials include a wide range of experimental and density functional theory (DFT) data, while for the binary one we prepared the DFT fitting database only. It consists of formation enthalpies and equilibrium volumes for the set of model structures with different coordination numbers, some of which included Ti-vacancy complexes.

The developed potential accurately describes properties from the fitting database, especially equilibrium volume, indicating high quality of the optimization procedure. It predicts the binding energies of complexes of point defects with up to three Ti atoms in bcc V in satisfactory agreement with DFT results. Elastic moduli of several model and experimentally observed structures are reproduced only qualitatively. However, these properties were not included in the optimization procedure. The POT_TiV potential predicts the melting point for the series of alloys with Ti concentration 60-80 % with overestimation of $\sim$ 19 % compared to the thermodynamic assessment. In turn, it predicts thermal expansion for the V-20Ti alloy almost perfect with a small underestimation at high temperatures. Calculated directly from the sum of the squares of atomic displacements, the diffusion coefficients show a decrease for V-4Ti alloy compared to pure V in all considered temperature range, which agrees with the fact of attractive interactions between Ti atoms and vacancies. And finally, molecular dynamics simulations of excess vacancies in pure V and V-4Ti alloy demonstrate that the addition of Ti prevents the formation of the vacancy loop and preserves the presence of individual vacancies as part of Ti-vacancy complexes.

Thus, the developed potential is less suited for studying diffusion and melting properties in equiatomic and Ti-enriched Ti-V alloys due to the mediocre description of their homologous temperature. Meanwhile, it can be successfully applied for studying any properties of V-rich alloys (with Ti concentrations $<$ 20 at. %) with emphasis on structure and energetics of radiation-induced point defect complexes. Finally, the proposed potential can be used for the development of other multi-component potentials, which include the Ti-V system as one of the component parts.

[1] Smith D, Chung H, Loomis B and Tsai H C 1996 *Journal of nuclear materials* **233** 356–363 URL `https://doi.org/10.1016/S0022-3115(96)00231-0`

[2] Zinkle S, Matsui H, Smith D, Rowcliffe A, Van Osch E, Abe K and Kazakov V 1998 *Journal of nuclear materials* **258** 205–214 URL `https://doi.org/10.1016/S0022-3115(98)00269-4`

[3] Zinkle S J, Möslang A, Muroga T and Tanigawa H 2013 *Nuclear Fusion* **53** 104024 URL `https://doi.org/10.1088/0029-5515/53/10/104024`

[4] de la Rubia T D, Zbib H M, Khraishi T A, Wirth B D, Victoria M and Caturla M J 2000 *Nature* **406** 871–874 URL `https://doi.org/10.1038/35022544`

[5] Loomis B, Smith D and Garner F 1991 *Journal of nuclear materials* **179** 771–774 URL `https://doi.org/10.1016/0022-3115(91)90202-I`

[6] Boev A, Aksyonov D, Kartamyshev A, Maksimenko V, Nelasov I and Lipnitskii A 2017 *Journal of Nuclear Materials* **492** 14–21 URL `https://doi.org/10.1016/j.jnucmat.2017.04.046`

[7] Hua J, Liu Y L, Li H S, Zhao M W and Liu X D 2015 *Computational Condensed Matter* **3** 1–8 URL `https://doi.org/10.1016/j.cocom.2015.03.004`

[8] Fellinger M R and Wilkins J W 2008 Embedded Atom Method Potential for Titanium-Vanadium Alloys *2008 APS March Meeting. Session D38: Metals: Defects and Elasctic properties* (Louisiana: APS) p 1 URL `http://meetings.aps.org/link/BAPS.2008.MAR.D38.3`

[9] Feng C, Peng X, Fu T, Zhao Y, Huang C and Wang Z 2017 *Physica E: Low-Dimensional Systems and Nanostructures* **87** 213–219 ISSN 13869477 URL `https://doi.org/10.1016/j.physe.2016.10.019`

[10] Yang X, Hu J and Jiang W 2019 *The European Physical Journal D* **73** 238 ISSN 1434-6060 URL `https://doi.org/10.1140/epjd/e2019-100387-9`

[11] Fu J, Li X, Johansson B and Zhao J 2017 *Journal of Alloys and Compounds* **705** 369–375 ISSN 09258388 URL `https://doi.org/10.1016/j.jallcom.2017.02.103`

[12] Boev, Anton and Nelasov, Ivan and Maksimenko, Vyacheslav and Lipnitskii, Aleksey and Saveliev, Valery and Kartamyshev, Andrey 2017 Molecular dynamics simulations of the excess vacancy evolution in v and v-4ti *Defect and Diffusion Forum* vol 375 (Trans Tech Publ) pp 153–166URL `https://doi.org/10.4028/www.scientific.net/DDF.375.153`

[13] Lipnitskii, AG and Saveliev, VN 2016 *Computational Materials Science* **121** 67–78URL `https://doi.org/10.1016/j.commatsci.2016.04.008`

[14] Kim Y M, Lee B J and Baskes M 2006 *Physical Review B* **74** 014101 ISSN 1098-0121 URL `https://doi.org/10.1103/PhysRevB.74.014101`

[15] Lee B J, Baskes M, Kim H and Koo Cho Y 2001 *Physical Review B* **64** 184102 ISSN 0163-1829 URL `https://doi.org/10.1103/PhysRevB.64.184102`

[16] Boev A, Lipnitskii A, Nelasov I, Saveliev V, Kartamyshev A, Maksimenko V and Zolnikov K 2017 Molecular dynamic simulations of the interaction of interstitial atoms with vacancy complexes in v and v-4ti *AIP Conference Proceedings* vol 1909 (AIP Publishing) p 020018 URL `https://doi.org/10.1063/1.5013699`

[17] Boev A O, Zolnikov K P, Nelasov I V and Lipnitskii A G 2018 *Letters on materials* **8** 263–267 URL `https://doi.org/10.22226/2410-3535-2018-3-263-267`

[18] Boev, AO and Zolnikov, KP and Nelasov, IV and Lipnitskii, AG 2019 Molecular dynamics simulation of primary radiation damage in vanadium and alloy v-4ti *Journal of Physics: Conference Series* vol 1147 (IOP Publishing) p 012087URL `https://doi.org/10.1088/1742-6596/1147/1/012087`

[19] Kartamyshev, AI and Lipnitskii, AG and Saveliev, VN and Maksimenko, VN and Nelasov, IV and Poletaev, DO 2019 *Computational Materials Science* **160** 30–41URL `https://doi.org/10.1016/j.commatsci.2018.12.044`

[20] Maksimenko, V N and Lipnitskii, A G and Nelasov, I V 2019 *AIP Conference Proceedings* **2167** 020213URL `https://doi.org/10.1063/1.5132080`

[21] Lipnitskii, A G and Maksimenko, V N and Nelasov, I V and Kartamyshev, A I 2019 *AIP Conference Proceedings* **2167** 020197URL `https://doi.org/10.1063/1.5132064`

[22] Kohn W and Sham L J 1965 *Physical Review* **140** A1133 URL `https://doi.org/10.1103/PhysRev.140.A1133`

[23] Hohenberg P and Kohn W 1964 *Physical review* **136** B864 URL `https://doi.org/10.1103/PhysRev.136.B864`

[24] Blöchl P E 1994 *Physical Review B* **50** 17953 URL `https://doi.org/10.1103/PhysRevB.50.17953`

[25] Gonze X, Amadon B, Anglade P M, Beuken J M, Bottin F, Boulanger P, Bruneval F, Caliste D, Caracas R, Cote M *et al.* 2009 *Computer Physics Communications* **180** 2582–2615 URL `https://doi.org/10.1016/j.cpc.2009.07.007`

[26] Kresse G and Furthmüller J 1996 *Computational Materials Science* **6** 15–50 URL

https://doi.org/10.1016/0927-0256(96)00008-0
[27] Aksyonov D, Fedotov S, Stevenson K and Zhugayevych A 2018 *Computational Materials Science* **154** 449–458 URL https://doi.org/10.1016/j.commatsci.2018.07.057
[28] Perdew J P, Burke K and Ernzerhof M 1996 *Physical review letters* **77** 3865 URL https://doi.org/10.1103/PhysRevLett.77.3865
[29] Methfessel M and Paxton A 1989 *Physical Review B* **40** 3616 URL https://doi.org/10.1103/PhysRevB.40.3616
[30] Monkhorst H J and Pack J D 1976 *Physical review B* **13** 5188 URL https://doi.org/10.1103/PhysRevB.13.5188
[31] (SGTE) 2012 Binary System Ti-V *Ternary Steel Systems: Phase Diagrams and Phase Transition Data* ed Franke P and Seifert H J (Berlin, Heidelberg: Springer Berlin Heidelberg) pp 62–62 ISBN 978-3-540-88141-4 URL https://doi.org/10.1007/978-3-540-88142-1_53
[32] Andersen H C 1980 *The Journal of Chemical Physics* **72** 2384 ISSN 00219606 URL https://doi.org/10.1063/1.439486
[33] Berendsen H J C, Postma J P M, van Gunsteren W F, DiNola A and Haak J R 1984 *The Journal of Chemical Physics* **81** 3684 ISSN 00219606 URL https://doi.org/10.1063/1.448118
[34] Nose S 1984 *Molecular Physics* **52** 255–268 ISSN 0026-8976 URL https://doi.org/10.1080/00268978400101201
[35] Vinet P, Ferrante J, Smith J and Rose J 1986 *Journal of Physics C: Solid State Physics* **19** L467 URL https://doi.org/10.1088/0022-3719/19/20/001
[36] Ziegler, J and Biersack, J and Littmark, U 1985 *Stopp. Range Ions Solids* **1** 109–140
[37] Marchukova L, Matveeva N and Kornilov I 1975 *Izv. VUZ Tsvetn. Metall.* 131–134
[38] Rudy E 1969 Ternary phase equilibria in transition metal-boron-carbon-silicon systems. part 5. compendium of phase diagram data Tech. rep. DTIC Document
[39] Ming L C, Manghnani M and Katahara K 1981 *Acta Metallurgica* **29** 479–485 URL https://doi.org/10.1016/0001-6160(81)90071-7
[40] Poletaev D, Lipnitskii A, Kartamyshev A, Aksyonov D, Tkachev E, Manokhin S, Ivanov M and Kolobov Y R 2014 *Computational Materials Science* **95** 456–463 URL https://doi.org/10.1016/j.commatsci.2014.08.010
[41] Fisher E and Renken C 1964 *Physical Review* **135** A482 URL https://doi.org/10.1103/PhysRev.135.A482
[42] Aksyonov D, Lipnitskii A and Kolobov Y 2012 *Computational Materials Science* **65** 434–441 ISSN 09270256 URL https://doi.org/10.1016/j.commatsci.2012.08.014
[43] Petry W, Heiming A, Trampenau J, Alba M, Herzig C, Schober H and Vogl G 1991 *Physical Review B* **43** 10933–10947 ISSN 0163-1829 URL https://doi.org/10.1103/PhysRevB.43.10933
[44] Han S, Zepeda-Ruiz L A, Ackland G J, Car R and Srolovitz D J 2003 *Journal of applied physics* **93** 3328–3335 URL https://doi.org/10.1063/1.1555275
[45] Brandes E 1983 *Smithells metals reference book, sixth edition*
[46] Maier K, Peo M, Saile B, Schaefer H E and Seeger A 1979 *Philosophical Magazine A* **40** 701–728 ISSN 0141-8610 URL https://doi.org/10.1080/01418617908234869
[47] Touloukian Y S, Kirby R K, Taylor R E and Desai P D 1975 *Thermophysical Properties of Matter - the TPRC Data Series. Volume 12. Thermal Expansion Metallic Elements and Alloys* (New York: IFI/Plenum)
[48] Takahara, Wataru 2014 *IOP Conference Series: Materials Science and Engineering* **61** 012029 ISSN 1757-8981URL https://doi.org/10.1088/1757-899X/61/1/012029
[49] Schultz H 1991 V *Atomic Defects in Metals* (Berlin/Heidelberg: Springer-Verlag) pp 173–178 URL https://doi.org/10.1007/10011948_53
[50] Woo C and Singh B 1990 *physica status solidi (b)* **159** 609–616 URL https://doi.org/10.1002/pssb.2221590210
[51] Brommer P, Béland L K, Joly J F and Mousseau N 2014 *Physical Review B* **90** 134109 URL https://doi.org/10.1103/PhysRevB.90.134109
[52] Fan Y, Kushima A, Yip S and Yildiz B 2011 *Physical review letters* **106** 125501 URL https://doi.org/10.1103/PhysRevLett.106.125501
[53] Stukowski A 2009 *Modelling and Simulation in Materials Science and Engineering* **18** 015012 URL https://doi.org/10.1088/0965-0393/18/1/015012
[54] Stukowski A, Bulatov V V and Arsenlis A 2012 *Modelling and Simulation in Materials Science and Engineering* **20** 085007 ISSN 0965-0393 URL https://doi.org/10.1088/0965-0393/20/8/085007
[55] Gao J, Cui L and Wan F 2016 *Materials Characterization* **111** 1–7 ISSN 10445803 URL https://doi.org/10.1016/j.matchar.2015.11.006
[56] Matsui H, Fukumoto K, Smith D, Chung H M, Van Witzenburg W and Votinov S 1996 *Journal*

of nuclear materials **233** 92–99 URL https://doi.org/10.1016/S0022-3115(96)00331-5

[57] Leguey T, Pareja R and Hodgson E 1996 *Journal of Nuclear Materials* **231** 191–198 URL https://doi.org/10.1016/0022-3115(96)00373-X